Chapter 7. Kolsky Compression Bar Experiments at High/Low Temperatures

When the specimen temperature differs from the room temperature, timing of mechanical load becomes a variable due to heat conduction. There are two approaches to conduct experiments with the specimens heated or cooled. One is to heat/cool the specimen with the bars attached. The other is to bring the bars in contact with the specimen after it reaches a desired temperature. The latter is preferred particularly at very high temperatures since temperature gradient in the bars affects wave propagation, which must be corrected. This chapter describes methods for high/low temperature Kolsky-bar experiments. The design of a computer-controlled automated system for high temperature experiments is presented. Examples are given with specimen materials including a stainless steel, a shape memory alloy, a syntactic epoxy foam, and PMDI foams with different densities.

7.1 Heating/Cooling the Specimen

The selection of heating and cooling devices depends on the specimen materials under investigation and the desired testing conditions. For example, to simulate the conditions of rapid heating together with high strain rates encountered in high-speed machining situations, fast heating of the metallic specimen can be achieved by passing high-intensity electrical current through the specimen. In a Kolsky compression bar developed at National Institute of Standard and Technology (NIST) (Mates et al. 2008), the heating rate in the specimen by the electrical current can be as high as 6,000 K/s. Mechanical loading is applied immediately after the heating to plastically deform the specimen at strain rates up to 10^4 s^{-1}. By contrast, many brittle materials, such as most glasses and ceramics, thermal shocks generated by rapid heating may cause damage and failure in the specimen before mechanical load is applied. In the experiments where the microstructure needs to be preserved for further microscopic analysis, a specimen at high temperature after high-rate deformation must be quenched at a specific time (Song et al. 2010). In most experiments at high or low environmental temperatures, the specimens are heated or cooled in such a way that the temperature in the specimen is nearly in equilibrium.

W.W. Chen and B. Song, *Split Hopkinson (Kolsky) Bar: Design, Testing and Applications*, Mechanical Engineering Series, DOI 10.1007/978-1-4419-7982-7_7,

The heating of the specimens may be supplied by electrical current (Basak et al. 2004; Mates et al. 2008) or focused infrared radiation (Lennon and Ramesh 1998) at high heating rates, furnace (Frantz et al. 1984) or environmental chambers at lower heating rates. Inductive heating (Rosenberg et al. 1986) and other in-house built heaters have also been used. When heating to high temperatures, a heating environment with an inert gas, such as argon or nitrogen, is desired to reduce the surface oxidation of the specimen. High-rate cooling may be achieved by immersing the specimen in a liquid already at desired temperature. Cooling at lower rates can be achieved in various environmental chambers. If possible, a thermal couple attached on the specimen is desired to record the actual temperature history in the specimen. Figure 7.1 shows a commercial furnace with an opening for the specimen to enter and exit. Many such furnaces are available with precise temperature control systems. Figure 7.2 shows a sketch of an in-house built environmental system (Song et al. 2005d). The system has an open hole for the test section of the Kolsky bar. The heating elements in the system are used for high-temperature experiments; whereas, flow rate of liquid nitrogen through the coil pipe creates a low-temperature environment in the opening at a desired low temperature.

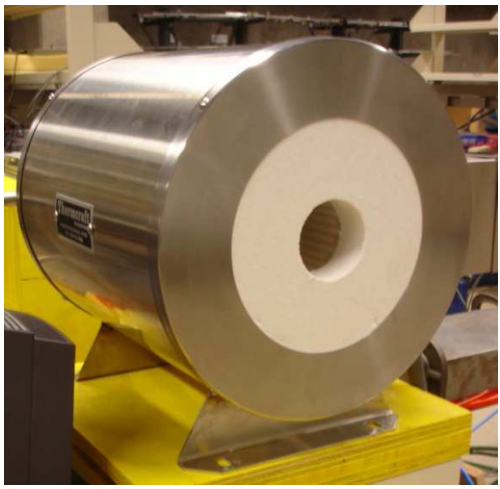

Figure 7.1 A commercial furnace to heating specimens

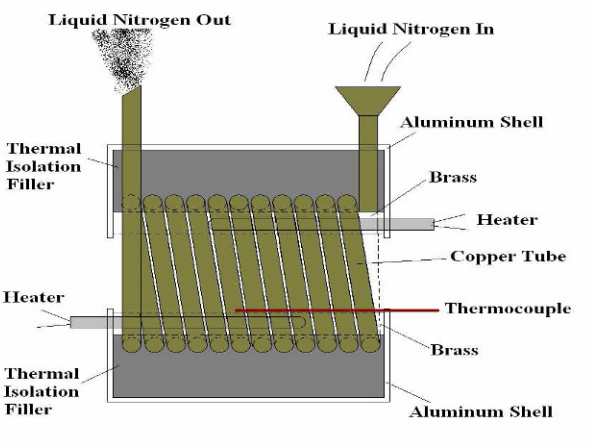

Figure 7.2 An example of in-house built environmental chamber
(Reproduced from Song et al. (2005d) with permission)

In the experiments with specimen temperatures differing from room temperature, timing of mechanical loading becomes a parameter that needs to be controlled in the experiments since heat can diffuse over time and alter the temperature and its distribution in the specimen. The main heat conduction path is through the metallic pressure bars. There are two approaches for the bars to be in contact with the specimens. One is to maintain constant contact between the bars and the specimen while the specimen is being heated up. This approach heats up the specimen and the bar ends together. Since the far ends of the bars are nearly at room temperature, there are temperature gradients along the bar axes. Depending on the desired temperature in the specimen, this temperature gradient may affect the wave propagation along the bar in a significant way. Chiddister and Malvern (1963) might have been the first to discuss the wave reflection and transmission in the bars with thermal gradients. The temperature gradients must be measured and the effects of the thermal gradients must be numerically corrected, particularly when the temperature is 600˚C or higher in steel bars. Figure 7.3 shows the effect of temperature on the modulus of elasticity for Inconel 718 steel (Seo et al. 2005). When the temperature is 600˚C or higher, the modulus of elasticity drastically decreases. Hence, the temperature gradient in the steel bar results in the gradient of modulus of elasticity. Changes in wave imped-

ance in terms of modulus of elasticity in the steel bar leads to disturbance to stress wave propagation. In addition, the exposure of the bar ends to high temperatures may anneal the bar material, which needs to remain elastic during the experiments. Due to these limitations, the direct-contact approach is not commonly used in compression experiments unless the temperature is not very high, such as those encountered in the characterization of polymers.

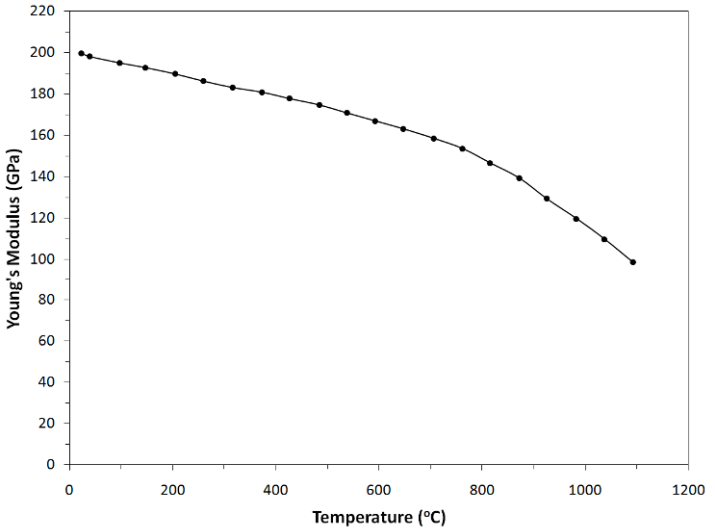

Figure 7.3 Effect of temperature on modulus of elasticity
(Reproduced from Seo et al. (2005) with permission)

The other approach is to expose the specimen to the temperature environment only. The bar ends are moved into contact with the specimen only shortly before the stress-wave loading. In this approach, when the room-temperature bar ends touch the hot/cold specimen, heat exchanges start immediately between the specimen and the bars. This leads to non-uniform temperature distribution on the specimen. The specimen temperature also changes instantly. One solution to keep the specimen at the desired and evenly distributed temperature is to add platens on both sides of the specimen. The platens can be the same material and diameter

as the bars or a temperature resistant material with impedance matching with that of the bars to minimize their disturbance to the wave propagation. The platens are in contact with the specimen and in the same environment chamber or furnace such that they have the same temperature as the specimen during the heating/cooling process. When the room-temperature bars are moved into contact with the platens, there are severe temperature gradients inside the platens. If the stress-wave loading is applied sufficiently quickly, the changes in the temperature and its distribution in the specimen are minimal. Due to the severe temperature gradients in the platens, the wave propagation through the platens may be affected, which is difficult to model and correct. However, the platens are typically thin enough that the entire specimen/platen test section assembly may be subjected to dynamic stress equilibrium through proper pulse shaping. Attempts to find the temperature distribution inside the platens through numerical simulations have been documented (Shazly et al. 2004).

The above challenges are usually encountered in high temperature Kolsky-bar experiments. Cold contact time (CCT) has been defined as the time during which the hot specimen stays in contact with the cold bars until being dynamically loaded. A short CCT is certainly desired in high-temperature Kolsky bar experiments. Experimental methods have been developed to facilitate relatively short CCT in high-temperature Kolsky-bar experiments. Frantz et al. (1984) developed an electric screw driven system to bring the bars into contact with the specimen pre-heated in a furnace. This design facilitates CCT as short as 400 ms with less than 5ºC decrease in specimen temperature. The design by Lennon and Ramesh (1998) can control the CCT to be as short as 1-2 ms. In their design, both the incident and transmission bars are initially separated from the hot specimen. An electropneumatic actuation system pushed the bars in contact with the specimen. In the following section, we will introduce an automated system that can adjust short CCT through precise timing control.

7.2 An Automated System for Precise Timing Control

From the descriptions in Chapter 7.1, it is obvious that, even with platens as temperature buffers, the specimen temperature will inevitably change when platens are in contact with the cold bars for an extended period of time waiting for the stress wave to arrive at the specimen. Ideally, the

stress waves should arrive immediately upon the contact between the bars and the specimen such that the temperature field in the specimen is nearly undisturbed. Alternatively, the stress wave should arrive at a fixed delay time after the contact such that heat exchange between the specimen and the bars is consistent. Both requirements (immediate loading or at a fixed delay) need precise control of the timing of the stress-wave arrival, which is difficult to achieve by manual operations. This section introduces an automated system to realize the required loading consistency in the Kolsky-bar experiments involving high/low temperatures, which was originally developed by Kuokkola and his students (Apostol et al. 2003).

The set-up is fully automated through controls over a series of pneumatic valves by a computer program. The mechanism of the automated control system is illustrated in Fig. 7.4 (Apostol et al. 2003). An environmental chamber or a furnace is used to set or change the specimen temperature. A pneumatically operated specimen manipulator is placed directly aiming at the opening of the environmental chamber or furnace. The specimen holder that is attached to the front of the manipulator places the specimen into the environmental chamber or furnace and then brings the specimen back to the test section with its centerline aligned with that of the bars after being retrieved from the temperature device. The transmission bar manipulator then moves the transmission bar towards the incident bar after the specimen is placed in the test section. A pneumatic circuit controls all the manipulators and valves, a pressurized air supply through software programming. To protect the temperature environment inside the chamber, the opening can also be covered by a door that is controlled by another pneumatic valve through the computer program.

In an experiment with this system, the specimen, together with its platens, is placed on the specimen holder. The specimen assembly is then fed into the environmental chamber or furnace through the opening for specimen. Temperature control is turned to a desired value prescribed in the computer program. A thermal couple attached on the specimen holder monitors the temperature variation on the specimen. While the temperature is on its way to the desired level, the striker is pushed into the gun barrel and the pulse shaper installed on the impact end of the incident bar. The gas gun chamber is filled with gas to necessary pressure. When the temperature reaches at a desired level in equilibrium, the thermal couple signal triggers the computer program to activate a valve to pull the specimen assembly out of the chamber/furnace and place the assembly in the test section of the Kolsky bar. Another valve is then turned on to activate the transmission bar manipulator to move the transmission bar towards the specimen and then push the specimen assembly in con-

tact with the incident bar, sandwiching the specimen assembly in the test section. The transmission-bar manipulator allows the transmission bar to move under stress-wave loading. The holding force is just sufficient to overcome the friction to move the transmission bar forward when activated by the computer program. While the pressure bars are being pushed together, the third valve launches the striker from the gas gun towards the pulse shaper on the impact end of the incident bar. Since the timing between all the operations is controlled by the computer program, the repeatability of the experiment is significantly improved, which is important in Kolsky-bar experiments when the specimen temperature is different from the ambient temperature. Figure 7.5 shows the main features of this system installed around the test section of a compression Kolsky bar. A close-up look at the specimen holder is shown in Fig. 7.6.

Figure 7.7 shows an experimental record of a dynamic high-temperature test using the system. In this figure, trace #1 indicates that, after heated to a desired temperature, the specimen assembly has returned to the test section. A position detector sends this signal signifying the proper positioning of the specimen. Trace #2 indicates that the transmission bar is in contact with the hot specimen assembly. Trace #3 signifies that the transmission bar has pushed the specimen assembly to be in contact with the incident bar. At this moment, the test section is ready to be loaded by the incident pulse of the Kolsky bar. Trace #4 is the strain gage signal from the incident bar surface. The time between Traces #3 and #4 can be adjusted in the computer program. In the specific example shown in Fig. 7.7, it takes about 42 ms for the stress wave to arrive at the specimen after it is sandwiched by the bars. The unique advantage of this automated system is that this time interval can be adjusted. Once the desired interval is determined, the system can repeat this interval from experiment to experiment, providing the necessary control over timing of loading in Kolsky-bar experiments at high/low temperatures.

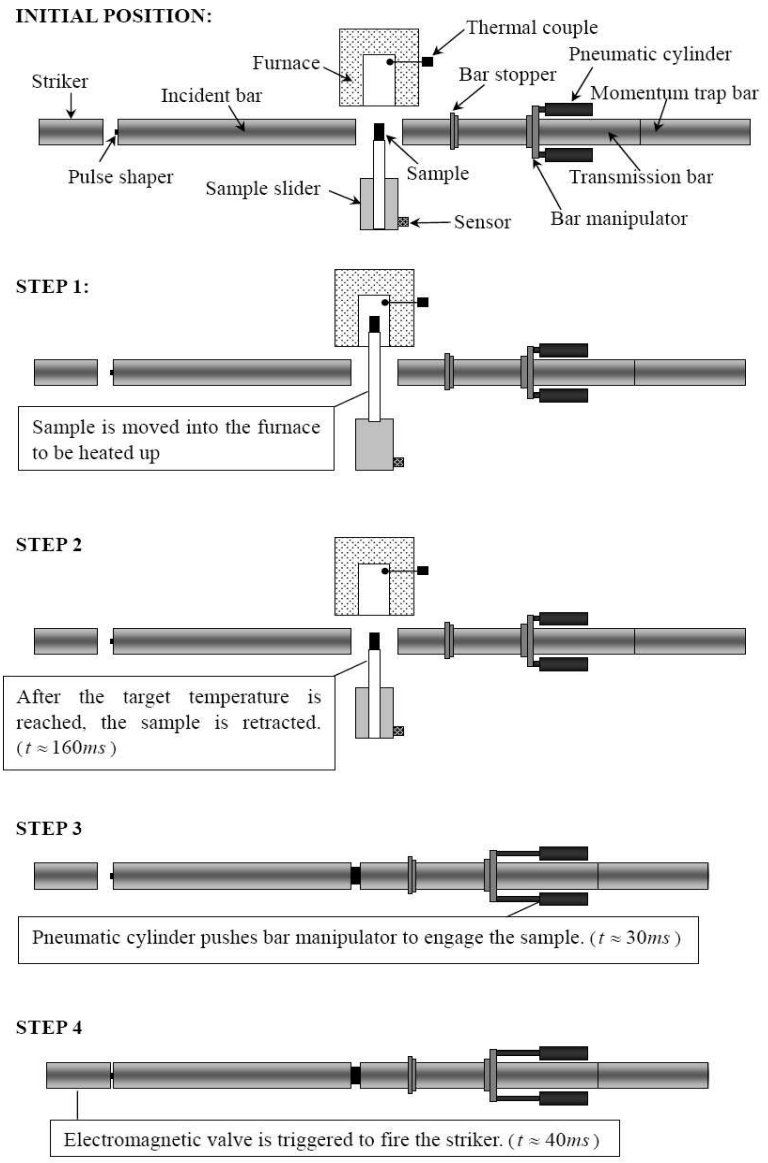

Figure 7.4 The automated control system

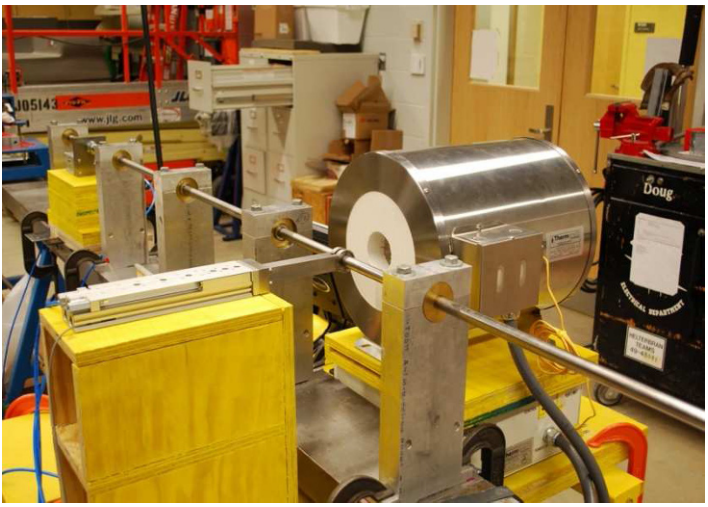

Figure 7.5 An automated system for high-temperature Kolsky bar experiments

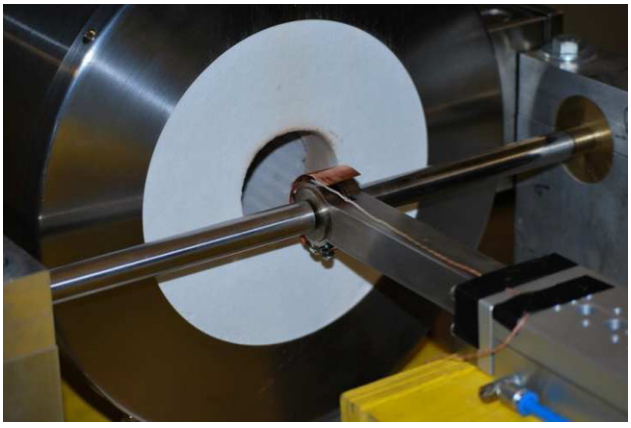

Figure 7.6 Details of the specimen holder

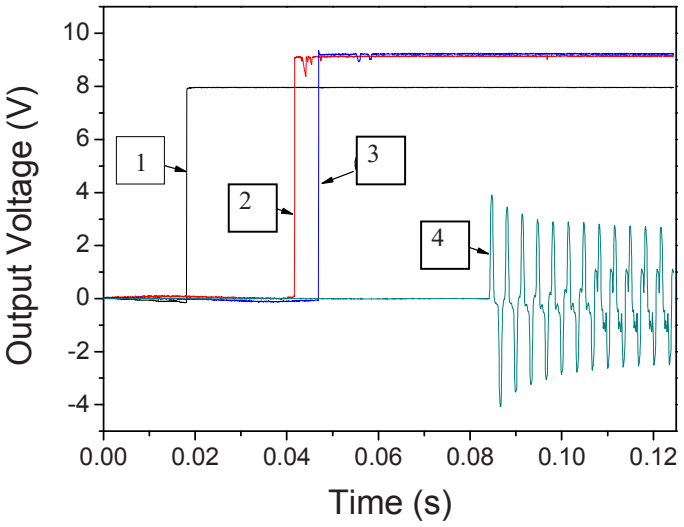

Figure 7.7 An experimental record illustrating the action sequence of a high-temperature compression Kolsky bar experiment

7.3 High Temperature Experiments on a Stainless Steel

The automated control system in Chapter 7.2 is one of the efficient approaches for high temperature Kolsky-bar experiments. However, other methods are also feasible as long as the specimen temperature is consistent during dynamic loading. In the following example of high temperature experiments on a 304L stainless steel, a Kolsky compression bar without the automated control system was used. The temperature history of each specimen was individually monitored.

The high-rate compressive response of 304L stainless steel was characterized at two elevated temperatures, 819˚C and 929˚C at a common strain rate of ~2500 s^{-1} (Song et al. 2010). The specimen assembly consists of two platens with the specimen in between. The assembly was heated before stress-wave loading while the bars remain at room temperature to avoid the temperature-gradient effect on the wave propaga-

tion in the bars. Upon contacting the cold bars, temperature gradients formed in the platens, leaving the temperature in specimen constant and uniform. Incident pulses are controlled with pulse shaping technique to produce constant strain-rate deformation and dynamic stress equilibrium in the specimen. In addition, a single loading feature was enabled such that recrystallization in the specimen can be related to the recorded histories of high-rate loading and high temperature. The mechanically loaded specimen was quenched into water at room temperature at 7 seconds or 30 seconds after loading to freeze the microstructures inside the specimen at different stages for further microscopic analysis. Dynamic recrystallization is one of the most important mechanisms for the microstructure evolution in materials with low to medium stacking fault energy to affect their macroscopic mechanical behavior. To ensure that recrystallization occurs in the specimen, the stainless steel specimens were compressed to large engineering strains over 0.5 at high rates and high temperatures.

A 19.05-mm-diameter C350 maraging steel Kolsky compression bar was used to conduct the high-rate characterization of the 304L stainless steel at elevated temperatures. The incident and transmission bars were 2388- and 1791-mm long, respectively. A 610-mm-long striker was used to generate an approximately 245-μs-long incident pulse, which can compress the specimen to the engineering strains over 0.5 at the strain rate of ~2500 s^{-1}. The cylindrical 304L stainless steel specimens had an initial diameter of 6.35 mm and length of 3.20 mm. The steel platens on both sides of the specimen were each 19.05 mm in diameter and 6.35-mm thick. The incident pulse was shaped using a 3.2-mm-diameter, 0.4-mm-thick annealed C11000 copper disk stacked on a 6.4-mm-diameter, 3.2-mm-thick M-2 tool steel disk to generate a nearly non-dispersive incident pulse that had an extended rise time for early stress equilibrium in the specimen and a flat plateau for constant engineering strain rate in the specimen. A liquid water-based glass suspension Deltaglaze 152 material was used as the high temperature lubricant to minimize the interfacial friction.

To monitor the temperature history of the specimen during the entire experiment duration, an OMEGA® K-type thermocouple was attached on the specimen surface. This thermocouple measured specimen temperature during pre-heating, dynamic loading, and post-load quenching stages of the experiment. The thermocouple had a 30-gage diameter. The thermal mass is small enough to have a sufficient response time for the Kolsky-bar experiments.

The momentum trapping system presented in Chapter 2.6 was employed to ensure a single loading on the specimen. Figure 7.8 shows a schematic of the experimental set up with the momentum trapping sys-

tem (Song et al. 2010). Figures 7.9 shows detailed configuration of the testing section. The 304L stainless steel cylindrical specimen was held with a thin disk made of light-weight ceramic wool. The specimen assembly that consists of the 304L steel specimen supported by the ceramic wool and a pair of steel platens sandwiching the specimen is placed and aligned to the pressure bars with a semi-circular steel channel. Figure 7.10 shows the configuration of the specimen assembly. The thickness of the ceramic wool disk is less than half of the specimen thickness so that the ceramic wool disk will not be loaded in axial direction during the experiment. Moreover, the ceramic wool disk has a bigger hole than the steel specimen to avoid providing additional lateral confinement to the specimen during compression.

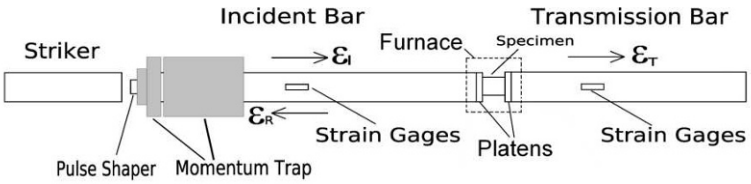

Figure 7.8 A schematic of the experimental setup for high-rate, high-temperature experiments
(Reproduced from Song et al. (2010) with permission)

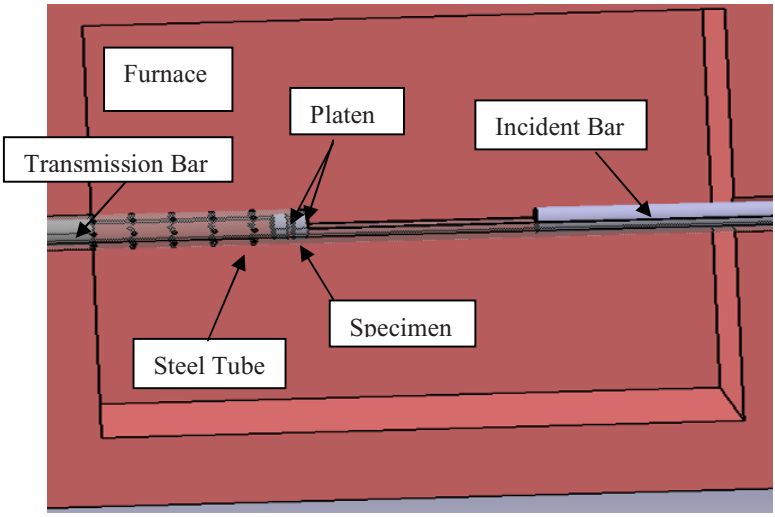

Figure 7.9 Configuration of the testing section
(Reproduced from Song et al. (2010) with permission)

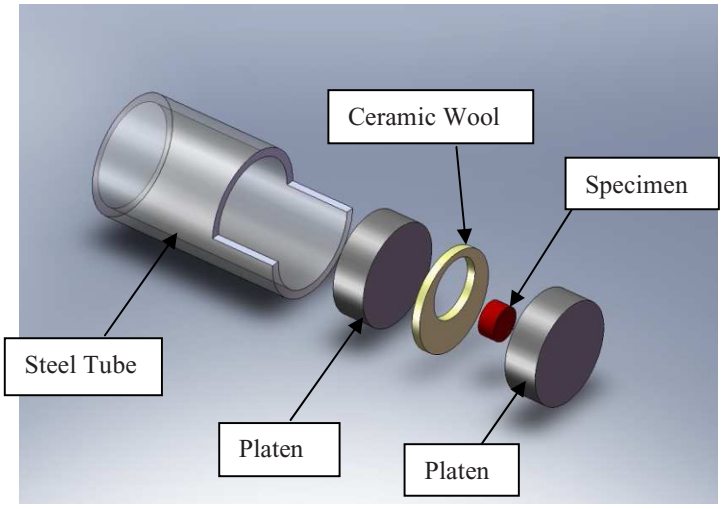

Figure 7.10 Configuration of specimen assembly
(Reproduced from Song et al. (2010) with permission)

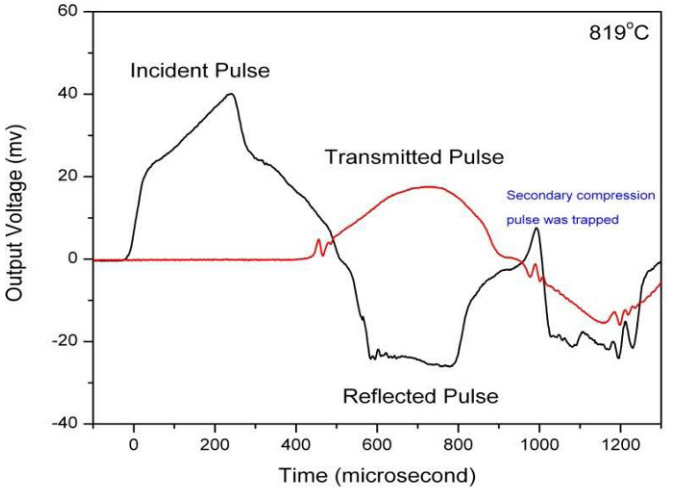

Figure 7.11 Experimental records of a high-rate, high-temperature experiment on 304L stainless steel
(Reproduced from Song et al. (2010) with permission)

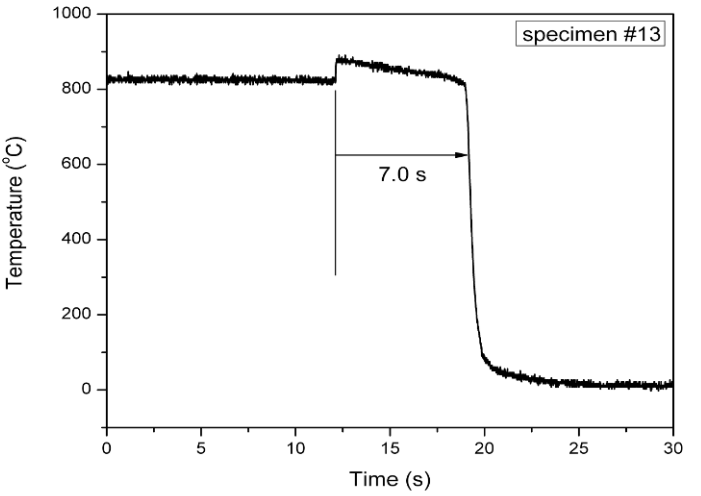

Figure 7.12 Temperature history in the specimen
(Reproduced from Song et al. (2010) with permission)

Figure 7.11 shows the incident, reflected, and transmitted pulses obtained from an experiment on the 304L stainless steel at an elevated temperature of 819ºC (Song et al. 2010). The figure shows that the profile-controlled incident pulse ensures the specimen in dynamic equilibrium during dynamic loading. Under stress equilibrium, the plateau in the reflected pulse shown in Fig. 7.11 represents the constant strain-rate history in the specimen. Furthermore, the secondary compressive wave was trapped and in turn changed to a tensile wave by using the momentum trap (Fig. 7.11). The specimen was thus loaded in compression only once.

Figure 7.12 shows the temperature history in the specimen measured with the thermocouple attached on the specimen surface over the entire experiment duration (Song et al. 2010). The temperature in the specimen was stabilized at 819ºC in the furnace. Then the specimen was dynamically compressed at the instant of 12th second. During dynamic compression, the temperature in the specimen rose from 819 ºC to 846ºC due to adiabatic heating from the plastic deformation in the specimen. Seven seconds after dynamic compression, the specimen was dipped into water for quenching, resulting in a sudden temperature drop at the instant of 19th second. Such complete thermal histories, together with the well-defined single loading history, are necessary to relate the microscopic recrystallization in the specimen to its thermal and mechanical loading histories.

Figure 7.13 shows a detailed temperature history in the specimen before and during dynamic compression, which is zoomed in for more details from Fig. 7.12. In this figure, the dynamic compression is set to start at time zero ($t = 0$). During dynamic compression, the specimen temperature increased with the increasing strain, or plastic work. The strain history is also shown in Fig. 7.13. Due to the short time duration of the dynamic loading, the energy available from plastic work adiabatically heated up the specimen, as discussed in Chapter 5.3.1. This adiabatic deformation produced an approximate temperature rise of 27 ºC in the specimen. The nearly linear history of strain in Fig. 7.13 also indicates that the specimen deformed at a constant strain rate of ~2450 s^{-1} to an engineering strain of 0.5.

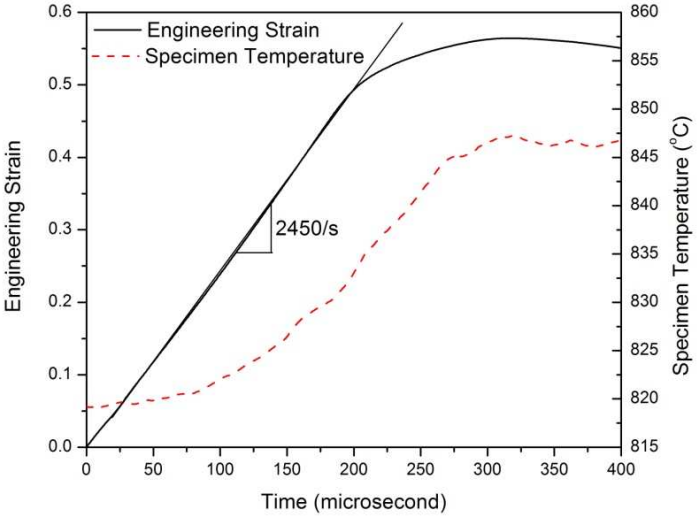

Figure 7.13 Strain and temperature histories in the specimen during dynamic compression
(Reproduced from Song et al. (2010) with permission)

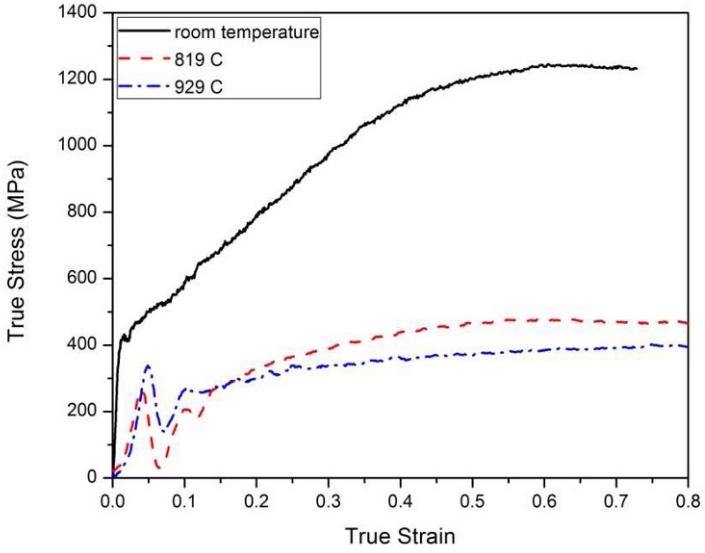

Figure 7.14 Dynamic compressive stress-strain curves of 304L stainless steel at various temperatures
(Reproduced from Song et al. (2010) with permission)

Following the same procedure, dynamic experiments on the 304L stainless steel were conducted at the same high strain rate but at another elevated temperature, 929 ºC. At this temperature, 7- and 30-second quenching times were carried out, respectively. Figure 7.14 summarizes the dynamic compressive stress-strain curves at the strain rate of 2450 s^{-1} at room temperature (23ºC), 819ºC, and 929ºC, respectively (Song et al. 2010). Due to employment of the long striker, the specimen was compressed to large deformation over 50% engineering strain. As shown in Fig. 7.14, temperature significantly affects the stress-strain response of the stainless steel. The flow stress at room temperature is nearly twice of that at elevated temperatures. It is noted that the stress-strain curves at both elevated temperatures exhibit oscillations at small strains, which is different from that obtained at room temperature. This may be due to the microstructure changes in the specimen at elevated temperatures. Furthermore, the microstructure changes are complex, resulting in mixed effects of temperature. The flow stress at large strains (>15%) at 819ºC is higher than that at 929ºC. However, when the strain is less than 15%, the flow stress at 819ºC is lower than that at 929ºC as shown in Fig. 7.14.

7.4 Temperature Effects on a Shape Memory Alloy

Phase transformation is a typical characteristic of shape memory alloys (SMAs). An SMA possesses an austenite phase at high temperatures and a martensitic phase at low temperatures, with a transition temperature in between. An SMA object appears to be permanently deformed at a low temperature in its martensitic phase. When it is heated to above the transition temperature of phase transformation, the alloy returns to its original shape in austenite phase. In addition to the temperature-induced phase transformations, martensitic transformation can also be induced by mechanical stress in a certain temperature range. In this temperature range, the austenite crystal structure in the stress-free alloy will transform into martensitic phase when an external stress exceeding the on-set stress for stress-induced martensite (SIM) is applied.

The temperature around the transition temperature of phase transformation for SMAs is of most interest. As an example of the same material introduced in Chapter 5.3.2, the SMA is NDC (Nitinol Devices & Components, Fremont, CA) SE508 which consists of 55.8% nickel by weight and the balance titanium. The austenite finish transition temperature is between 5 and 18ºC. The temperature range under investigation

here is set from 0 to 50ºC, covering the phase transformation transition temperature. Since the temperature is only 25 ºC above or below room temperature, the effect of temperature gradient on stress-wave propagation is negligible. The heating/cooling chamber shown in Fig. 7.2 was placed between the incident bar and the transmission bar (around the specimen) to control environmental temperatures.

The VascoMax maraging steel bars used for the experiments had a common diameter of 12.3 mm and lengths of 1830, 762, and 305 mm for the incident, transmission, and striker bars, respectively. In order to investigate the temperature effect on both loading and unloading stress-strain response of the SMA, the reverse pulse shaping technique presented in Chapter 2.6 was also implemented to the Kolsky-bar experiments. The front pulse shaping ensures the specimen deforms at constant strain rates under stress equilibrium while the rear pulse shaping unloads the specimen at the same constant strain rate. Except for the environmental temperature, the experimental procedure is the same as that presented in Chapter 5.3.2.

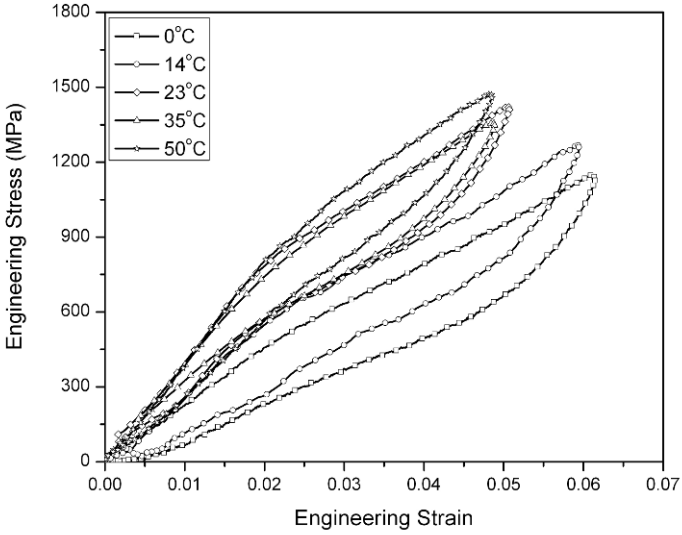

Figure 7.15 Dynamic stress-strain curves of the Nitinol SE508 at various temperatures
(Reproduced from Chen and Song (2006) with permission)

Figure 7.15 summarizes the dynamic compressive stress-strain curves at the strain rate of 430 s^{-1} for the Nitinol SE508 SMA at environmental temperatures of 0, 14, 23, 35, and 50ºC (Chen and Song 2006). Although the environmental temperature varied within a small range of 50 ºC, significant temperature effect was observed in the resultant stress-strain responses. As the environmental temperature decreases from 50 to 0ºC, the slopes of both the loading and unloading stress-strain curves decreased. When the environmental temperature is below room temperature, i.e., 14ºC and 0ºC, the strain does not return to zero, as indicated by the residual strain in the unloading stress-strain curves at these temperatures, even though the specimen has been completely unloaded. The specimen eventually recoverd all strains at room temperature. This phenomenon indicates that, under high-rate deformation, the reverse phase transformation needing thermal energy input may not be as fast as the forward SIM. When the environmental temperature is close to the phase transformation temperature, the heat is drawn from the specimen to assist the reverse transformation. The temperature in the specimen may drop below the phase transformation temperature during the unloading. The reverse transformation is consequently terminated unless more heat is drawn from the environment to drive the specimen temperature back above the transition temperature. It is also observed that, although 0ºC is below the transition temperature of phase transformation of the SMA, superelasticity is still reached. This indicates that the forward SIM driven by stress actually released heat into the specimen, resulting in the actual specimen temperature above the transition temperature of phase transformation during the superelastic deformation in the specimen.

7.5 Temperature Effects on an Epoxy Syntactic Foam

This set of experiments explores the effects of temperature on the dynamic compressive properties of a syntactic epoxy foam. The epoxy syntactic foam is the same material as described in Chapter 4.5.3.1, which had a glass transition temperature of 70ºC. The cylindrical specimens had a diameter of ~12.60 mm and a thickness of ~4.10 mm.

The Kolsky bar used was made of 7075-T6 aluminum alloy and had a common diameter of 19.05 mm. The incident, transmission, and striker bars were 2134-, 803-, and 305-mm long, respectively. Annealed C-11000 copper disks were used to shape the incident pulse to ensure nearly constant strain-rate deformation of specimens under dynamic

equilibrated stresses. The single-loading feature employed in the stainless steel experiments (Fig. 7.8) was also used on the aluminum bar to facilitate microscopic examinations on damage mode in the syntactic foam after loading.

Specimen temperature consists of adiabatic temperature rise during dynamic compression and environmental temperature. The environmental temperature is controlled by the environmental chamber. Unlike the stainless steel specimens that went through large strains at high rates, the adiabatic temperature rise in the epoxy syntactic foam specimens during dynamic compression is expected to be negligible. To verify this, a miniaturized thermocouple was embedded into the specimen to record the temperature history during dynamic loading. The T-type thermocouple with a low thermal mass and a small diameter of 75 μm was placed inside the specimen through a small hole. Since the specimen was damaged by the small hole for thermocouple before mechanical loading, the measurements of temperature rise therefore provided only an estimation of the adiabatic heating.

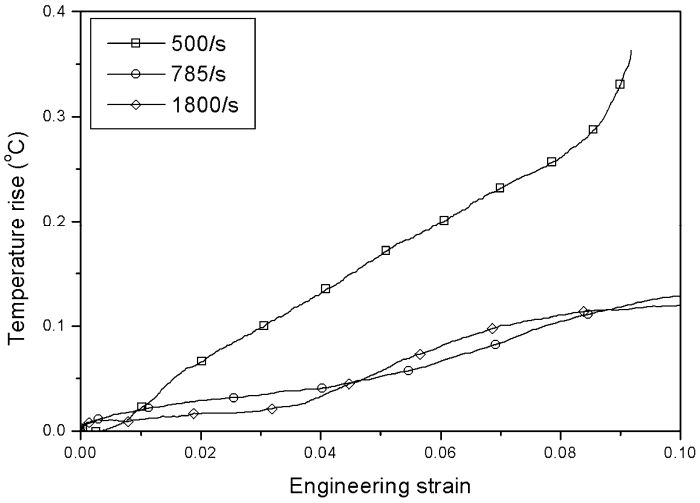

Figure 7.16 Adiabatic temperature rise in syntactic epoxy foam specimens deforming at different high rates
(Reproduced from Song et al. (2005d) with permission)

Figure 7.16 shows the temperature rise in the syntactic epoxy foam specimens as a function of engineering strain during dynamic compression at strain rates of 500, 785, and 1800 s^{-1}, respectively (Song et al. 2005d). The adiabatic temperature rise in the specimen is verified to be small in all three cases. Little heat was generated during dynamic compression because of the small failure strain and low failure strength of the epoxy syntactic foam. Although it is clear that the effects of adiabatic temperature rise in the syntactic foam specimen are negligible, it is interesting to note that the temperature rise at the strain rate of 500 s^{-1} is higher than that at the strain rates of 785 and 1800 s^{-1}. This phenomenon may be the result of a change in the failure/damage mechanism in specimen. The mechanical energy in the specimen during dynamic deformation is dissipated either through the formation and propagation of small cracks or through the generation of heat, or both. In a related study (Song et al. 2004b), it was observed that more microcracks formed in the foam specimen under higher-rate dynamic loading than under lower-rate dynamic loading. The mechanical energy in the specimen at higher dynamic strain-rate deformation was mostly dissipated through the formation and propagation of small cracks

To control the environmental temperature, a heating/cooling system schematically shown in Fig. 7.2 was placed between the incident bar and the transmission bar over the test section of the Kolsky bar. Since the temperature range of the syntactic foam in the most proposed engineering applications is expected to be approximately -55˚C to 75˚C, the temperatures at which the Kolsky-bar experiments were conducted at -54ºC, -25ºC, 0ºC, 23ºC(room temperature), 50ºC, and 74ºC, which spanned over the glass transition temperature of 70˚C for the epoxy syntactic foam.

The experimental procedure is the same as that described in Chapter 4.5.3.1. Figure 7.17 shows the resultant dynamic uniaxial compressive stress-strain curves at the temperatures of -54ºC, -25ºC, 0ºC, 23ºC, 50ºC, and 74ºC at the strain rate of 550 ±10% s^{-1} (Song et al. 2005d). In Fig. 7.17, unloading portions in the low temperature stress-strain curves (-54˚C and -25˚C) were recorded since the maximum strains achieved in both experiments were slightly below the failure strain. However, no unloading part was meaningful in the other stress-strain curves due to specimen failure. The stress-strain curves of the syntactic foam show that the material is strongly sensitive to environmental temperature at the same strain rate: the initial modulus of elasticity, maximum failure stress and the strain at maximum stress are all dependent on environmental temperature.

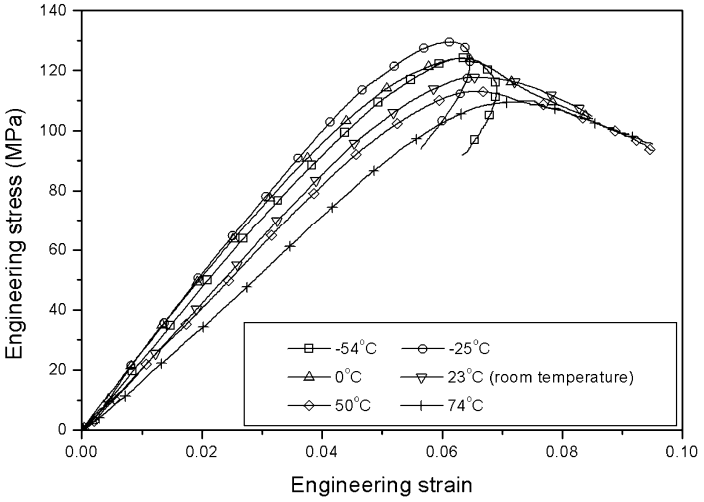

Figure 7.17 Dynamic compressive stress-strain curves at various temperatures *(Reproduced from Song et al. (2005d) with permission)*

Within the range of environmental temperature in this research, an approximate threshold temperature value of -25ºC separated the trends of temperature dependencies into two regions. When environmental temperature is above the threshold value (-25ºC), the stress-strain curves exhibit increasing initial modulus of elasticity and maximum failure strength, but decreasing maximum failure strain with decreasing environmental temperature at the same strain rate. However, when environmental temperature is below the threshold value, both the modulus of elasticity and maximum failure strength decreased with decreasing temperature. The maximum failure strain increased at the temperature of -54ºC in comparison to that at the temperature of -25ºC. The stress-strain curve at the temperature of -25ºC had the highest values of initial modulus of elasticity (2.60 GPa) and maximum failure strength (130 MPa), and the lowest value of maximum failure strain (6.1%) within the temperature range from -54ºC to 74ºC.

At a fixed strain rate, e.g., 550 s^{-1}, when environmental temperature was above the threshold temperature of -25ºC, thermal-softening may dominate the stress-strain behavior. However, when a specimen was in an environment with a temperature below -25ºC, damage-softening due to the formation and propagation of cracks in specimen dominates over the lower-temperature-induced hardening. It is also noted that, when the environmental temperature exceeded the glass transition temperature (70ºC) of the foam material, the initial modulus of elasticity did not exhibit significant decrease.

The specimens after mechanical tests were mounted into epoxy resin to examine the failure modes with optical microscopy. Due to the utilization of pulse shaping and single loading, specimens were loaded only once during dynamic compression. The failure modes preserved in the specimens after mechanical loading thus correspond to the well-defined loading history. Figures 7.18(a), (b), and (c) show the micrographs of the recovered specimens after mechanical tests at the same strain rate of 550 s^{-1} at various temperatures (0ºC, 23ºC, and 74ºC) (Song et al. 2005d). At a low temperature, e.g., 0ºC, a significant crack, which connected glass-microspheresites, was observed in the specimen, as shown in Fig. 7.18(a). This crack oriented ~45º to the loading axis. When the temperature rose to 23ºC, instead of significant cracks, some microcracks were formed through connecting a few glass microspheresites (Fig. 7.18(b)). As the temperature further close to 74ºC, less glass microspheresites were found to connect together (Fig. 7.18(c)). Most of glass microspheresites distributed in specimen separately (Fig. 7.18(d)), implying less microcracks in specimen at high temperatures. The results of micrographs in Fig. 7.18 indicate that the specimen exhibits brittle behavior at low temperatures, as indicated by the connecting microspheresites that leads to the formation of small cracks (Fig. 7.18(a)), but the failure mode changes at high temperatures where no connected microspheresites were observed (Figs. 7.18(c) and (d)).

To further investigate the effects of environmental temperature on dynamic compressive response of the foam, dynamic compressive experiments at the temperatures of 50ºC, 23ºC, 0ºC, and -54ºC at a higher strain rate of 1100/s were then conducted. The resultant dynamic compressive stress-strain curves are shown in Fig. 7.19 (Song et al. 2005d). The experimental results at this higher strain rate exhibited similar dependencies of the stress-strain behavior on environmental temperature as those at the strain rate of 550 s^{-1}.

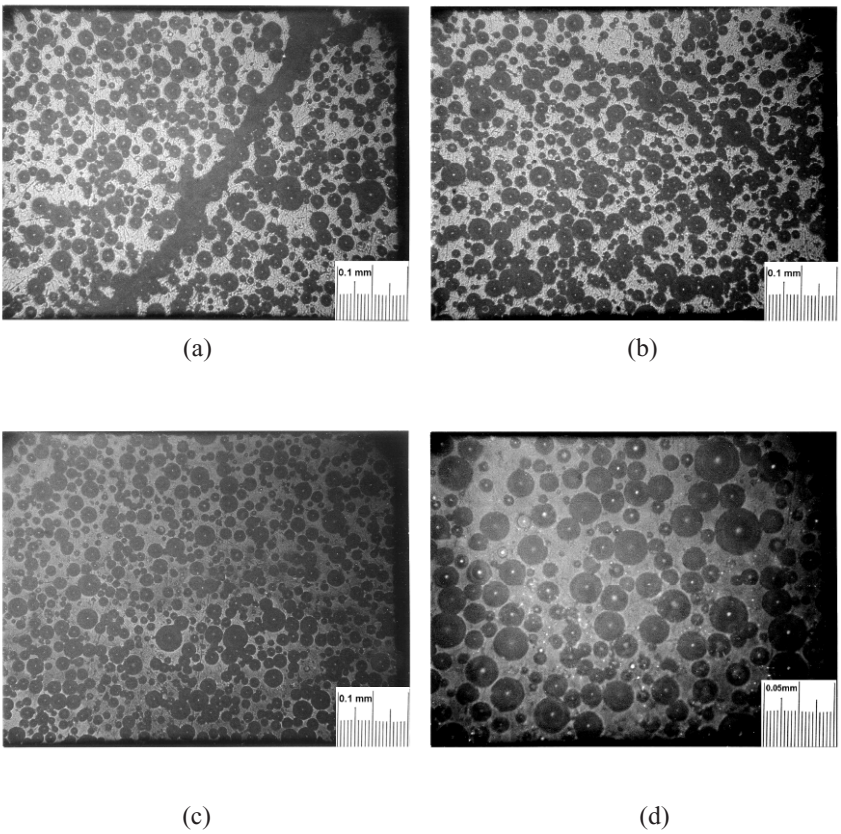

(a) (b)

(c) (d)

Figure 7.18 Failure modes in specimens
(a) 0ºC; (b) 23ºC; (c) 74ºC, 100X; (d) 74ºC 200X
(Reproduced from Song et al. (2005d) with permission)

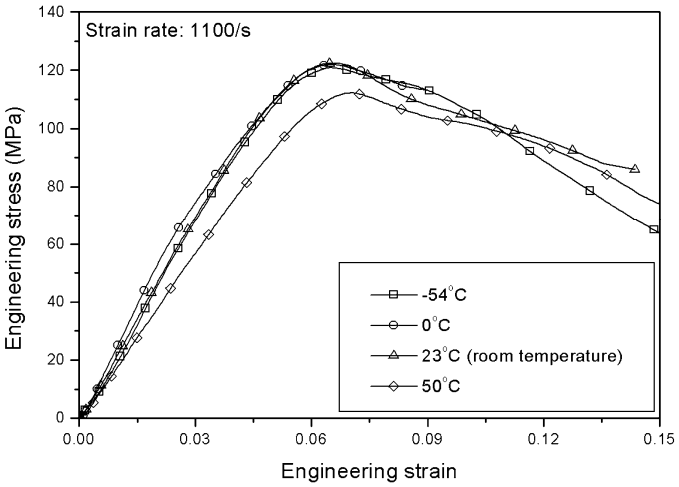

Figure 7.19 Dynamic compressive stress-strain curves at various temperatures (1100 s^{-1})
(Reproduced from Song et al. (2005d) with permission)

7.6 Temperature Effects on PMDI Foams

The compressive stress-strain response of the PMDI foam materials with different densities at room temperature has been described in Chapter 4.5.3.2. Here, we present the effects of temperature on the compressive response of the PMDI foam materials with three different densities (0.31×10^3, 0.41×10^3, and 0.55×10^3 kg/m^3). Dynamic compression experiments were conducted at various temperatures (-54ºC, -12ºC, 50ºC, 74ºC), in addition to room temperature (22 ºC). These experiments had a fixed dynamic strain rate of 3×10^3 s^{-1} (Song et al. 2009d).

The heating/cooling chamber shown in Fig. 7.2 was used to control temperature in the experiments. The temperature was the only variable in this set of experiments. Strain rate was maintained to be nearly identical for each density foam material. Figures 7.20, 7.21, and 7.22 show the compressive stress–strain curves of the foam materials with three differ-

ent densities at various temperatures (Song et al. 2009d). For foam materials with a certain density, temperature influences the plateau stress of the foam materials. For the materials with densities of 0.31×10^3 and 0.41×10^3 kg/m^3, the stress-strain curves do not significantly change in shape when the temperature varies (Figs. 7.20 and 7.21). However, the shape of the stress–strain curve for the 0.55×10^3 kg/m^3 foam material changes from low to high temperatures. As shown in Fig. 7.22, all of the stress–strain curves exhibited an ''N'' shape except for that obtained at the temperature of 347 K (74ºC). Instead, the stress–strain curve at 347 K exhibits a long plateau, which was similar to the curves obtained at low strain rates (Fig. 4.35(c)). The variation in the shapes of stress–strain curves was due to different deformation and collapse mechanisms at different temperatures. The material appears more brittle at lower temperatures, causing sudden collapse of the cell structures. At high temperatures, the foam material is more ductile, resulting in plastic buckling as the major deformation. Even under impact loading, the 0.55×10^3 kg/m^3 foam specimen still exhibited load-bearing capability at high temperatures.

We take the yield strength of the foam materials at various temperatures to determine the temperature effect more quantitatively. The results are shown in Fig. 7.23 (Song et al. 2009d). The yield strength increases with decreasing temperature for all three foam materials. However, the sensitivity of the yield strength to the temperature depends on the density of the foam material, as indicated by the different slopes in the temperature sensitivity curves in Fig. 7.23.

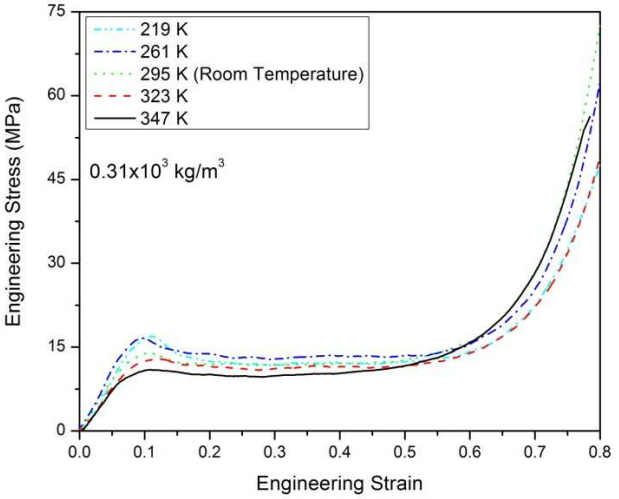

Figure 7.20 Stress-strain curves of 0.31×10^3 kg/m^3 foam at various temperatures
(Reproduced from Song et al. (2009d) with permission)

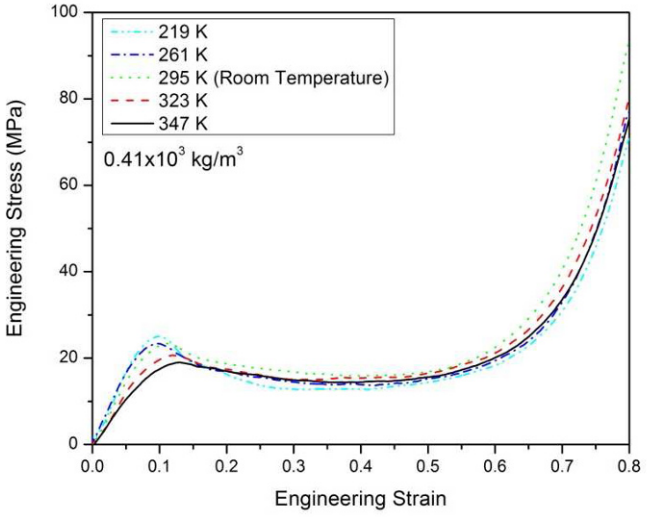

Figure 7.21 Stress-strain curves of 0.41×10^3 kg/m^3 foam at various temperatures
(Reproduced from Song et al. (2009d) with permission)

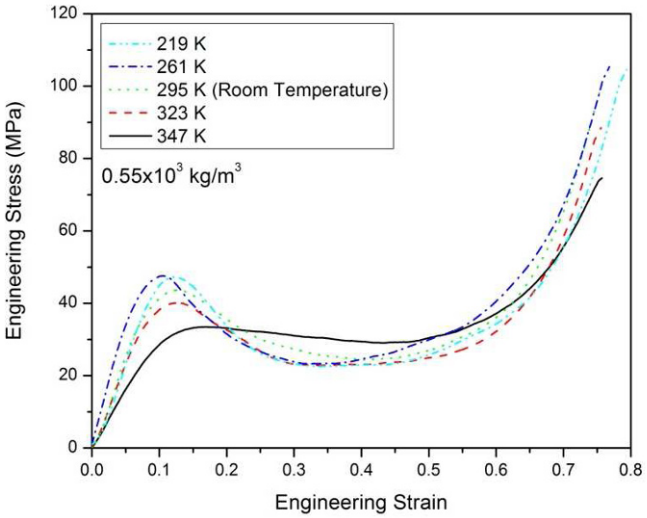

Figure 7.22 Stress-strain curves of 0.55×10^3 kg/m^3 foam at various temperatures
(Reproduced from Song et al. (2009d) with permission)

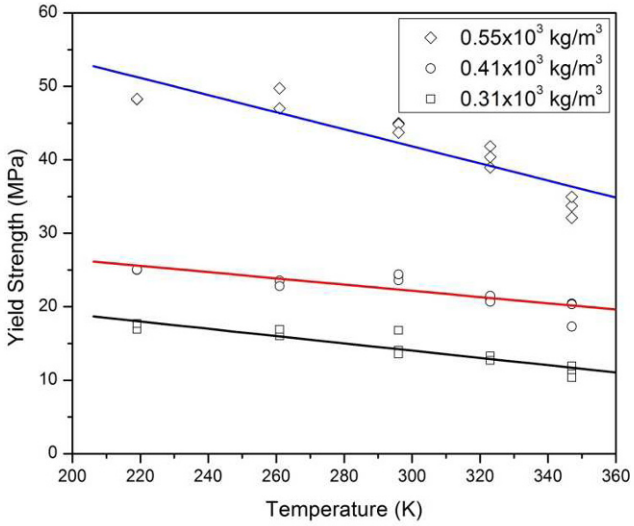

Figure 7.23 Temperature sensitivities of the foam materials with different densities
(Reproduced from Song et al. (2009d) with permission)